

Figure 1 Thermodynamic representation of the effect of high-entropy fluid removal on compression efficiency

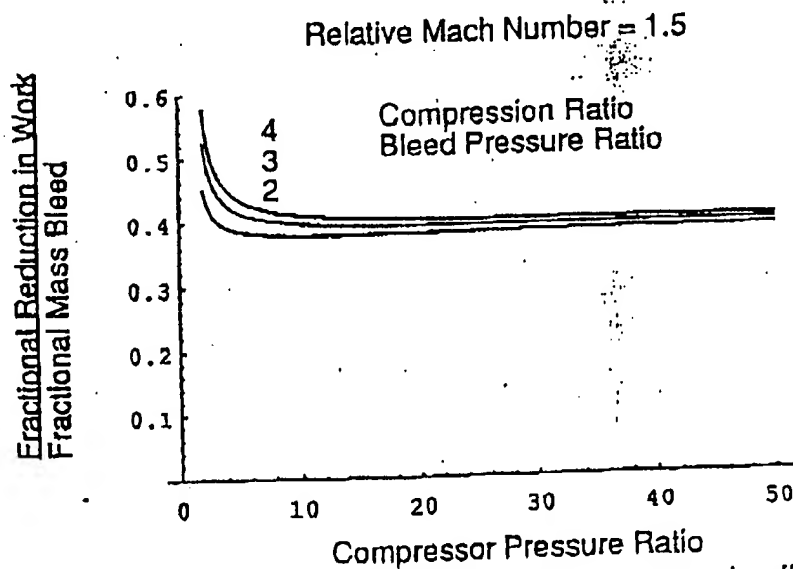
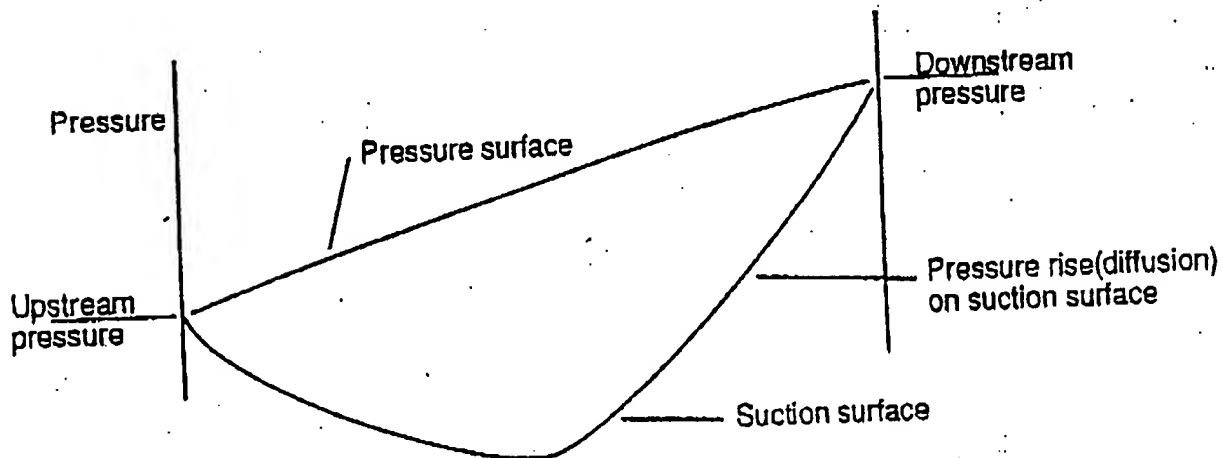
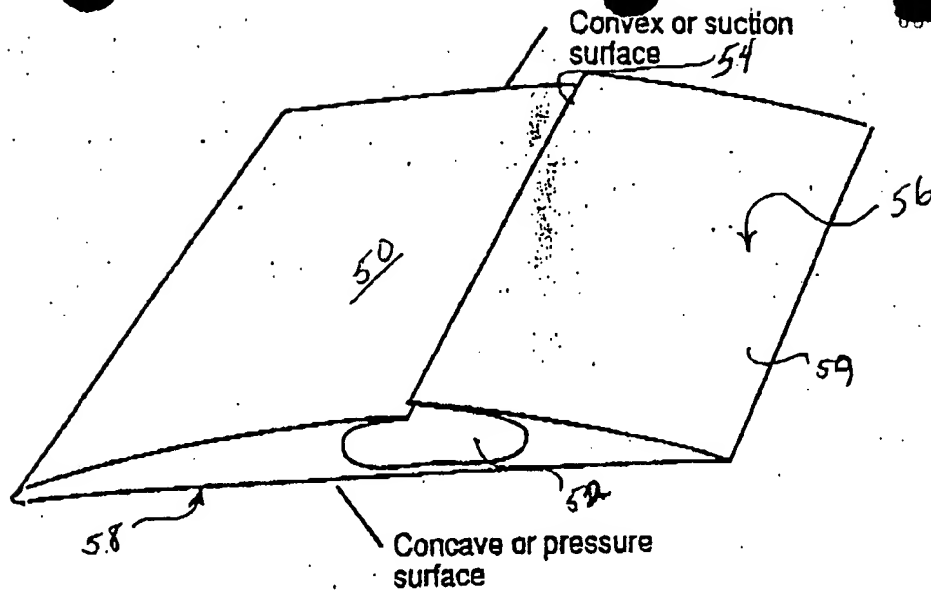


Figure 2 Fractional reduction in work (or fractional increase in efficiency) per fraction of fluid removed.

01/13/97

59383 U.S. PTO
08791057

FIG 3



08791057 011397

FIG 4

465070-45076280

59383 U.S. PTO
08791057
01/13/97

FIG 5

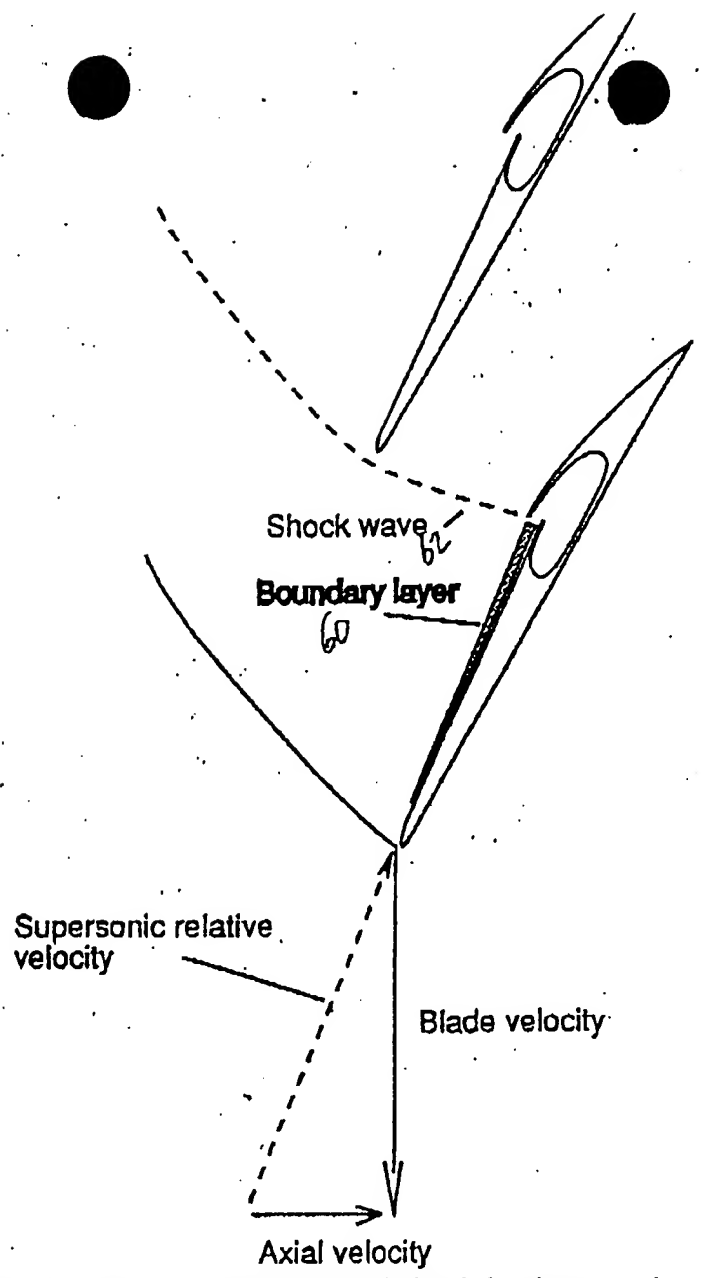


Figure 5 Illustrating fluid removal ahead of shock impingement

FIG 6

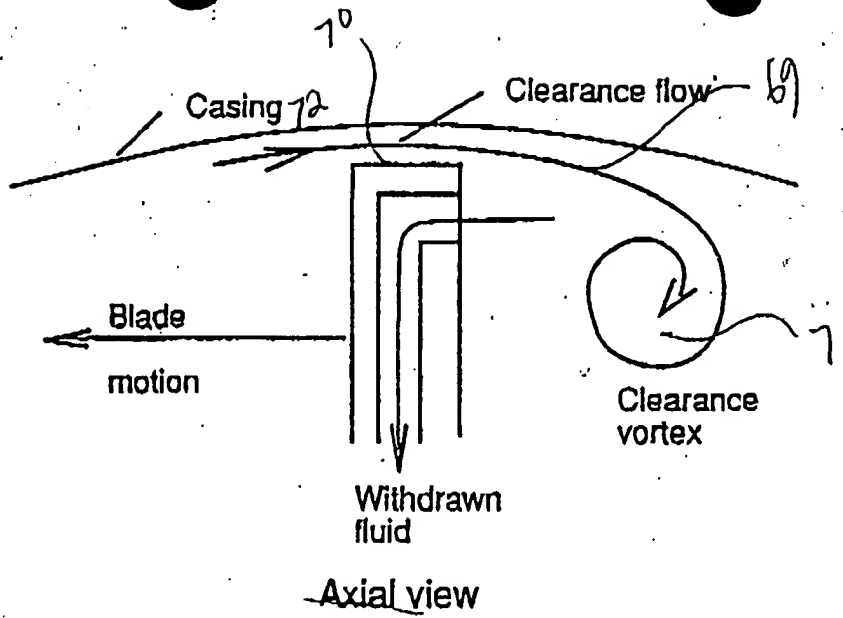
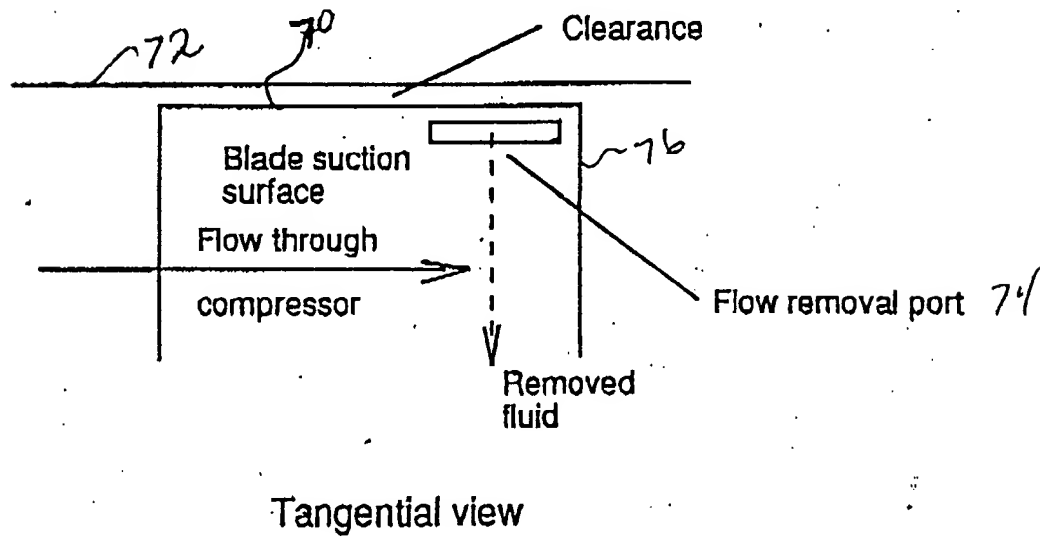
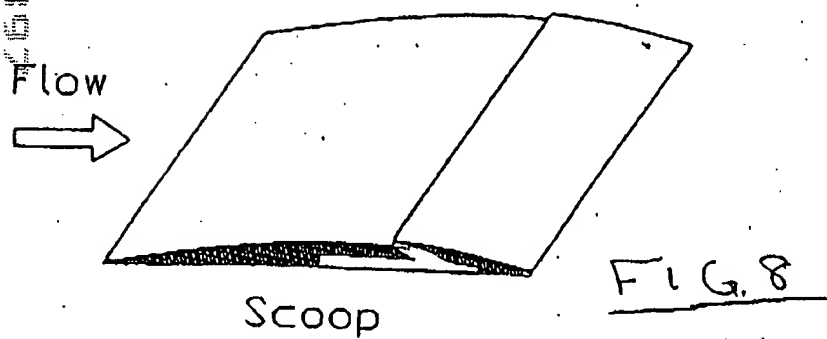
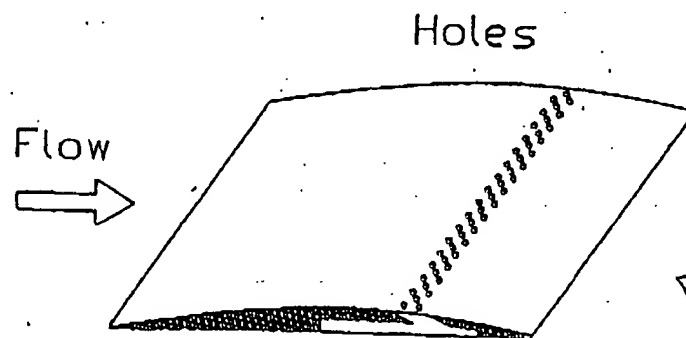
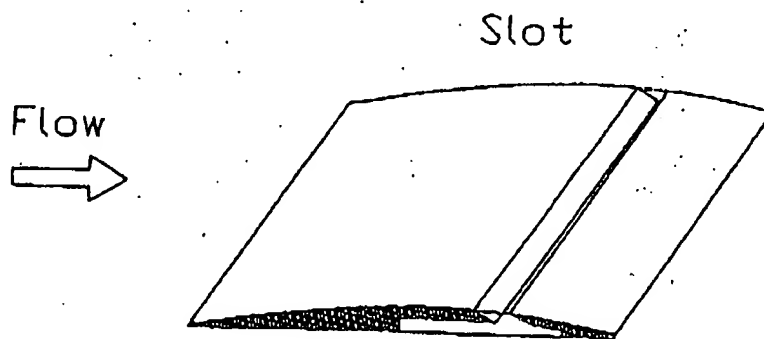


FIG. 7.



Illustrating fluid removal near trailing edge of suction surfact at blade tip, to negatve clearance vortex blockage.



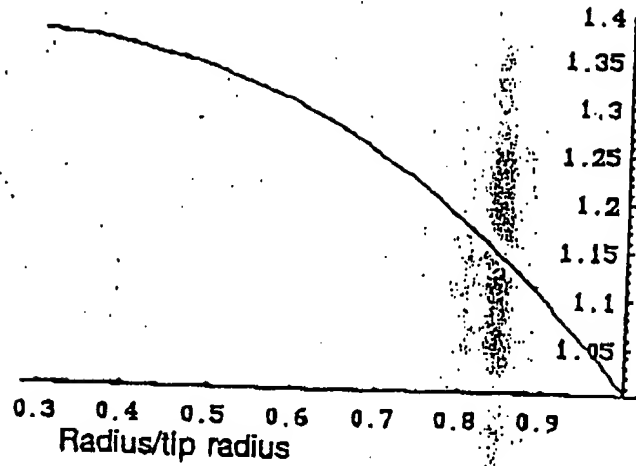


FIG 11

Figure 11 Variation with radius of ratio of blade-relative stagnation pressure to passage pressure

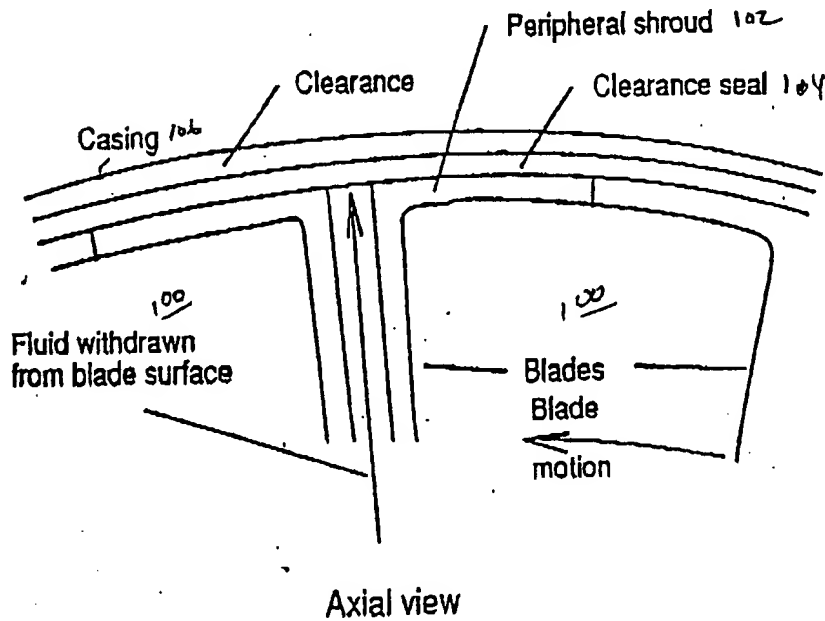


FIG 12

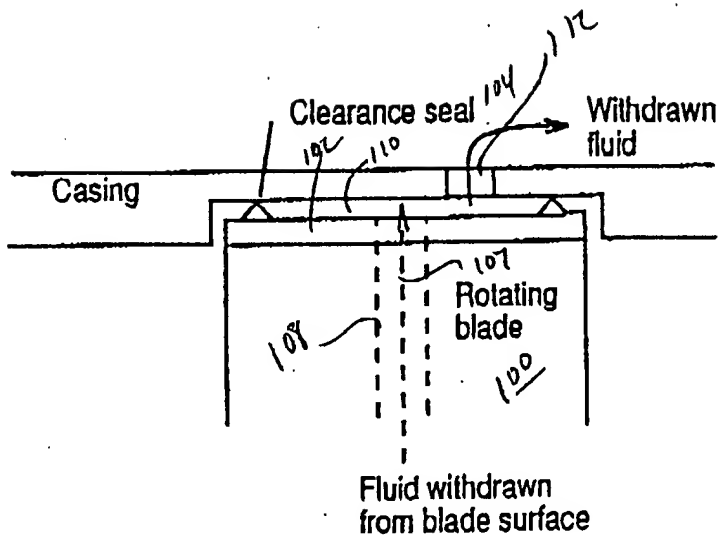
08791057-011397

59383 U.S. PTO

08791057



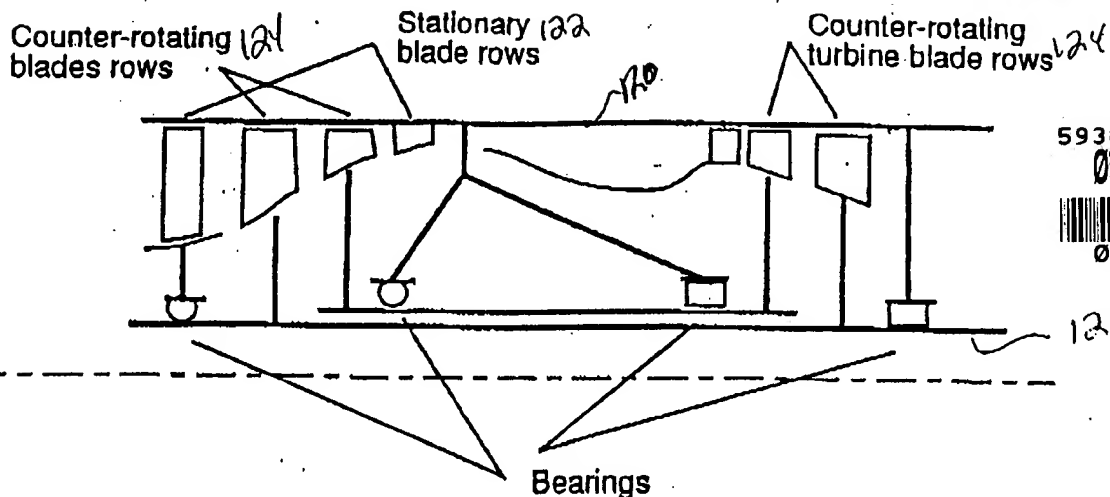
01/13/97



Tangential view

Fig 13

08791057



59383 U.S. PTO

08791057



01/13/97

Figure 14 Schematic arrangement of counter-rotating compressor with stationary blade rows upstream and downstream of counter-rotating pair..

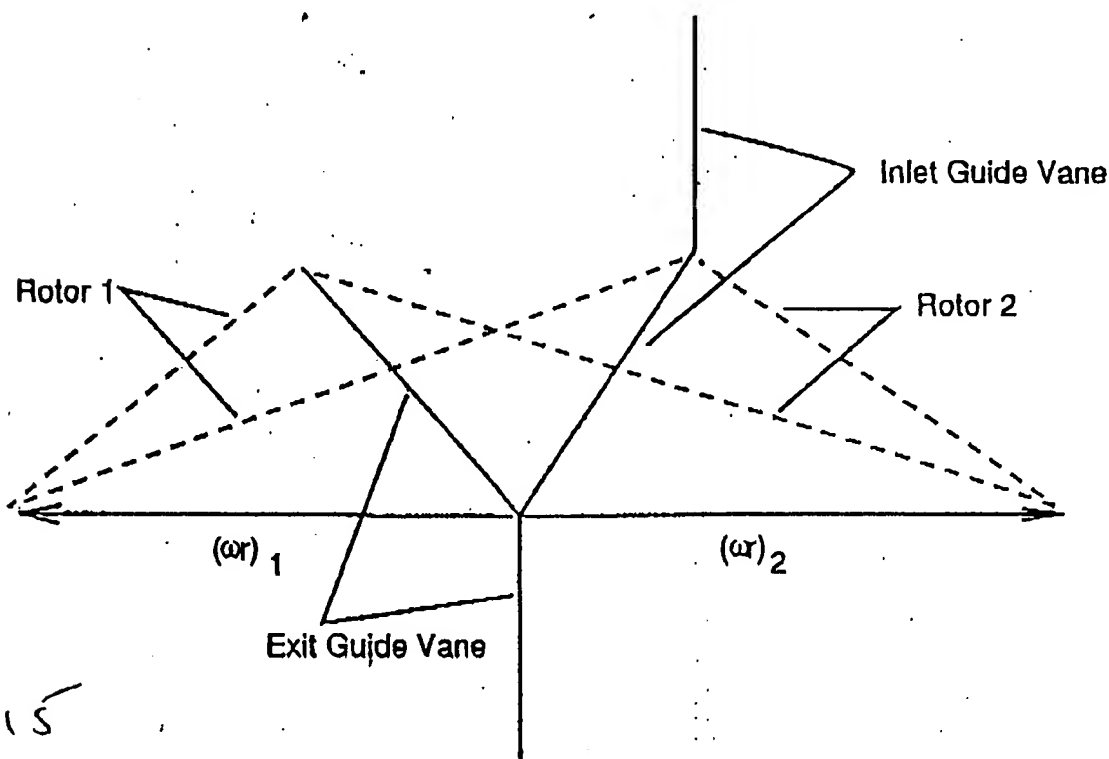


Figure 15 Velocity triangles for counter-rotating compressor with inlet and exit stator blades, and balanced diffusion in the two rotors.